Mon. Not. R. Astron. Soc. **419,** 706–712 (2012) doi:10.1111/j.1365-2966.2011.19732.x

More on the nature of the variable star UNSW-V-760

C. Koen★

Department of Statistics, University of the Western Cape, Private Bag X17, Bellville, 7535 Cape Town, South Africa

Accepted 2011 August 29. Received 2011 August 26; in original form 2011 July 14

ABSTRACT

The results of two multicolour time-series photometric observing runs, separated by about two months, are presented. The same periodicities previously detected in photometry of UNSW-V-760 are still present, albeit at substantially reduced amplitudes. Amplitudes also changed considerably between the two runs. A new periodicity, probably the second harmonic of one of the modes, has appeared. Flares were observed in one of the observing runs. All Sky Automated Survey photometry of the star shows overt variability over a limited time-span. The possibility is entertained that the properties can be explained by chance alignment of the K dwarf star with a distant blue pulsator.

Key words: stars: flare – stars: individual: UNSW-V-760 – stars: variables: general.

1 INTRODUCTION

The unusual variable star UNSW-V-760 (hereafter referred to as V760) was discovered in the course of the University of New South Wales search for extrasolar planetary transits (Christiansen et al. 2008). V760 was found to be periodic, with $P = 0.20$ d. Further observations and analysis by Koen (2011) showed that V760 is in fact multiperiodic: its variability is well explained by the two periods 0.1979 and 0.2756 d, and their first harmonics. He also presented standardized photometry and two spectra of the star, and deduced a classification of K1Vke–K3Vke.

Koen (2011) argued that at least one of the two periodicities, possibly both, should be due to pulsation of the star. If correct, V760 would be unique: to the best of the author's knowledge, there are no known pulsating main-sequence stars of types later than F. For example, in a recent study of solar-like oscillations discovered by the *Kepler* mission, it is noted that there is a paucity of pulsators with effective temperatures in the range 5300–5700 K, which separates the cooler evolved stars from the hotter main-sequence stars (Verner et al. 2011).

V760 is within the positional uncertainties of both *ROSAT* and *Einstein* X-ray detections. Given the sparsity of the field, and the fact that Ca emission is seen in the spectra, this suggests that the star is chromospherically active. However, no overt sign of flaring was seen in almost 36 h of intensive photometric monitoring, including 4.2 h in the *U* band.

In this paper, the results of further time-series photometry of V760 are presented, and an alternative explanation for its properties is discussed.

★E-mail: ckoen@uwc.ac.za

2 PHOTOMETRIC OBSERVATIONS AND REDUCTIONS

Observations were made at the South African Astronomical Observatory (SAAO) near Sutherland, South Africa. The observing log is given in Table 1. The STE4 CCD camera, attached to the 1.0-m telescope was used for the first extended observing run. The camera had a field of view of about 5×5 arcmin, hence there were several bright local comparison stars available. Pre-binning (2×2) was used throughout, giving a readout time of 20 s. During the first night, measurements were made through an Hα filter only; thereafter, observations cycled through *UBV* filters. Exposure times were tailored to observing conditions, which were generally quite good (photometric, with seeing of better than 1.5 arcsec).

Reductions were obtained online by an automated version of DOPHOT (Schechter, Mateo & Saha 1993). The programme and comparison stars are quite bright in *B* and *V*, and aperture photometry proved less noisy than brightnesses derived from point spread function (PSF) fitting. V760 is a late-type star, relatively faint in *U*, and hence PSF magnitudes were preferred for this filter. Similarly, the Hα filter is relatively narrow, hence the measured fluxes from the programme and comparison stars are small, and PSF magnitudes showed less scatter. The photometry was differentially corrected using the measurements of the two or three bright stars in the field of view with the smallest scatter in their observations.

Nightly *UBV* zero-points were set by the mean magnitudes of the three brightest stars in the field of view.

A second observing week followed two months later. Photometry was obtained with the STE3 camera, mounted on the SAAO 1.9-m telescope. The small field of view of 73×73 arcsec meant that only a single bright comparison star could be accommodated. Observing conditions were mostly good, and measurements could be made on all seven nights. Observations were obtained in *U* and *B* on every night, and *V* and *R* were sometimes included – see Table 1.

Table 1. The observing log. T_{exp} is the exposure time and N is the minimum number of useful measurements per filter obtained during a given run. The first night's observing was done through an Hα filter; for the remaining CCD runs, observing cycled through a selection from *UBVR*. The photoelectric photometry obtained with the 0.5-m telescope was in the *U* band only.

Telescope	Starting time (HJD 245 5000+)	T_{exp} (s)	Run length (h)	N
1.0 m	563.3966	90 (Hα)	4.7	165
	566.2985	100–120 (*U*), 15–30 (*B*), 9–10 (*V*)	7.4	124
	567.2872	100–130 (*U*), 20–30 (*B*), 8–12 (*V*)	7.9	139
	568.2854	60–100 (*U*), 15–20 (*B*), 7–8 (*V*)	7.7	167
	569.2823	100 (*U*), 15 (*B*), 7 (*V*)	7.8	151
	570.2806	100–120 (*U*), 15–20 (*B*), 7 (*V*)	7.5	128
0.5 m	600.3526	5 (*U*)	4.4	2866
1.9 m	630.3856	100 (*U*), 30 (*B*)	4.9	90
	631.2960	100–120 (*U*), 30 (*B*), 15 (*V*)	3.6	68
	632.2484	100–120 (*U*), 20–30 (*B*), 10–15 (*V*), 5–7 (*R*)	7.7	105
	633.2482	120 (*U*), 30 (*B*), 15 (*V*), 7–15 (*R*)	7.3	110
	634.2422	140 (*U*), 45 (*B*), 25 (*V*)	8.4	121
	635.2358	120–140 (*U*), 24–40 (*B*), 10–25 (*V*), 5–15 (*R*)	7.9	129
	636.2397	140 (*U*), 45–60 (*B*), 25–30 (*V*), 10–15 (*R*)	7.9	74

Reductions were as for the data acquired on the 1.0-m telescope, with PSF magnitudes used throughout, and all measurements referred to the single bright comparison star.

One short, high time resolution (5 s) run was obtained with the Modular Photometer attached to the SAAO 0.5-m telescope. The instrument is a photoelectric photometer with a GaAs tube. Measurements were made through the *U* filter only, under excellent photometric conditions and no moon background. The observations were corrected for the dark sky background illumination and air extinction.

For convenience, the 2010 SAAO observations analysed by Koen (2011) will be referred to as 'data set 1' below, while the two sets of 2011 observations will be named 'data set 2' (1.0-m measurements) and 'data set 3' (1.9-m data), respectively.

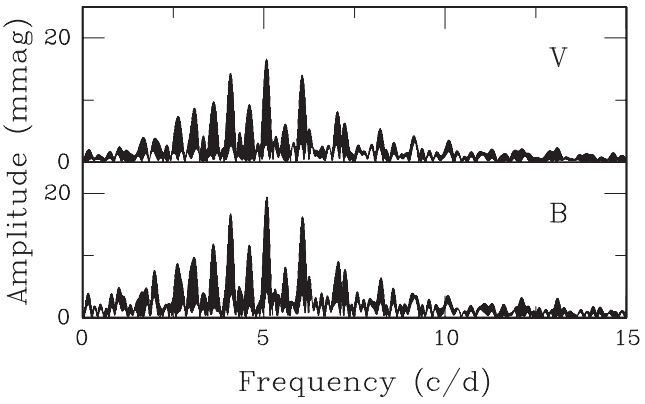

Figure 1. Amplitude spectra of the combined data sets 2 and 3 *V*- and *B*-filter observations.

3 DISCUSSION OF THE SAAO OBSERVATIONS

Koen (2011) fitted four frequencies to the photometry of V760 obtained by Christiansen et al. (2008) and by himself, namely 5.05336 and 3.62813 d^{-1}, and their first harmonics. The first point to consider is whether the combined data sets 2 and 3 are consistent with these frequencies. A preliminary look at amplitude spectra of the new data shows that there are indeed power excesses at frequencies close to all four of the prominent features in the earlier data (Fig. 1).

The detailed approach chosen was to first calculate the spectrum in a small interval around 5.05 d^{-1}, the most prominent frequency in the earlier data, and then to pre-whiten by the frequency associated with the largest amplitude in the interval. The amplitude spectrum of the residuals was then studied in the frequencies near 3.628 d^{-1}; the data pre-whitened by the most prominent frequency; and so on for the remaining two frequencies. The procedure is illustrated in Fig. 2, for the *V* filter data. Aliasing of the combined data, is, of course severe, due to the gap of several weeks between the two data sets – not to mention the gaps within the two sets of observations. Alias peaks are separated by 0.0147–0.0153 d^{-1} (roughly 1/68–1/66 d^{-1}). In all four cases the frequencies from Koen (2011) are within 0.005 d^{-1} of one of the four largest amplitude aliases in the amplitude spectra. This applies to both the combined *B* data sets, and the combined *V* data sets. This confirms that as far as the data allow conclusions to be drawn, these frequencies are still present in the latest measurements.

The spectra of the residuals left after pre-whitening by the four frequencies can be seen in Fig. 3. There are three sets of features of interest: first, peaks near 2 d^{-1} (maxima at 2.0071 d^{-1} in both *V* and *B*), and its 1 d^{-1} aliases. These are most probably artefacts caused by the slight zero-point mismatching of the differentially corrected data sets from different nights. Secondly, there is considerable residual power in the interval 3.5–8 d^{-1}, particularly near 5 d^{-1}, i.e. the vicinity of the principal frequency in the original data. This is caused by substantial differences in the amplitudes of variation seen in data sets 2 and 3. It is tempting to continue the frequency extraction process within this frequency interval, and hence to explain the variation in amplitude over the two months between the data sets as being due to the beating of very close frequencies. This would be pointless, as it could not explain the much larger amplitudes seen in data set 1. For the time being, it simply has to be accepted that there is substantial amplitude variation in V760, a point further demonstrated and discussed in Section 4.

The third feature in Fig. 3 to be remarked on is the peak near 13 d^{-1} (the maximum power is at 12.886 d^{-1}); its ± 1 d^{-1} aliases are also clearly visible. Interestingly, this is seen only in the *V*-filter

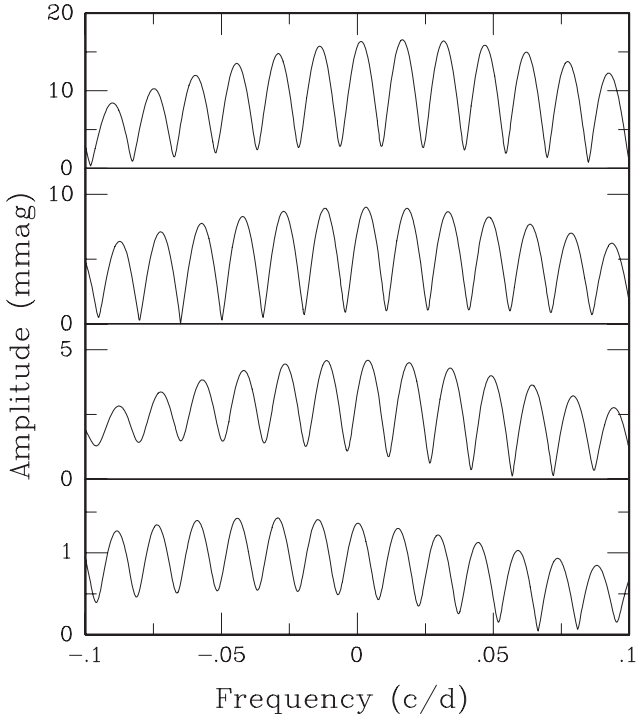

Figure 2. Details of the spectra around the frequencies 5.053, 3.628, 7.256 and 10.107 d^{-1} (from top to bottom). In each case, the combined data sets 2 and 3 *V*-filter data have been pre-whitened by the most prominent frequencies in the preceding panels of the figure.

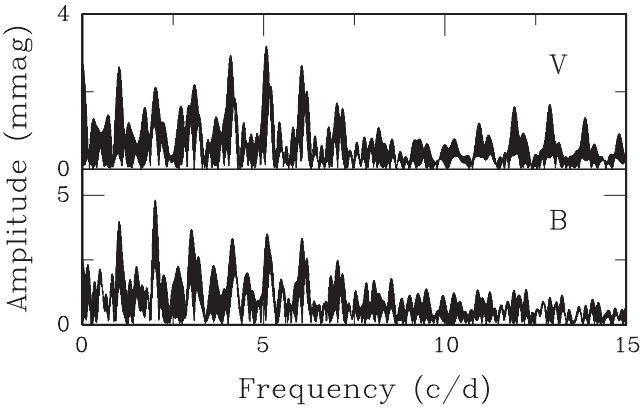

Figure 3. Amplitude spectra of the *V*-filter (top panel) and *B*-filter (bottom panel) residuals left after pre-whitening the combined data sets 2 and 3 observations by the four frequencies in Table 2.

data. Given that the data set 3 observations have been standardized by a single comparison star, and that the same star was also used (together with others) to differentially correct the data set 2 measurements, it is conceivable that this feature is caused by variability in the comparison star. This was ruled out by re-reducing data set 2, excluding the star in question as comparison, and noting that the peak near 13 d^{-1} remained in the V760 spectra. The possible new periodicity in the *V* data will be further discussed below.

The individual data sets 2 and 3 are now considered. Figs 4 and 5 show fits of the four data set 1 frequencies to the data set 2 *V* and *B* data. Two points are noteworthy: first, the nightly zero-points are those determined by local comparison stars, i.e. nightly data have not been shifted vertically in the plots to obtain the best possible fit. The fact that the data none the less closely follow the predicted

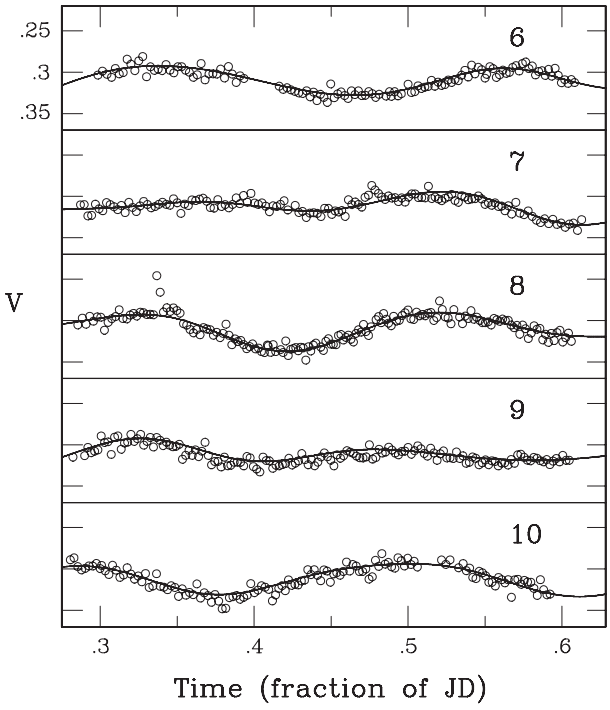

Figure 4. The data set 2 *V*-band photometry. The solid line shows the fit of the four previously known frequencies to the measurements. Each panel is labelled with the last digit of the Julian Day of the observations. Nightly magnitude zero-points were set by three bright stars in the field of view.

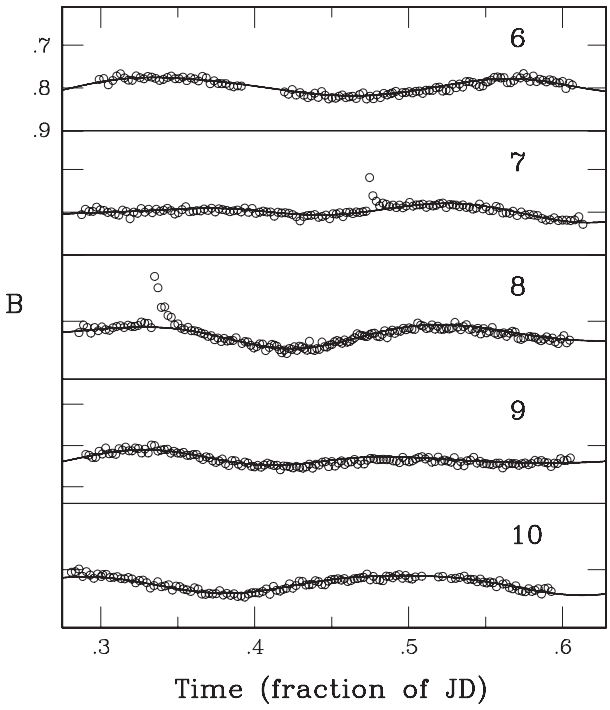

Figure 5. The data set 2 *B*-band photometry. The solid line shows the fit of the four previously known frequencies to the data. Each panel is labelled with the last digit of the Julian Day of the observations. Nightly magnitude zero-points were set by three bright stars in the field of view. Note the differences in the vertical scales used in Figs 4 and 5.

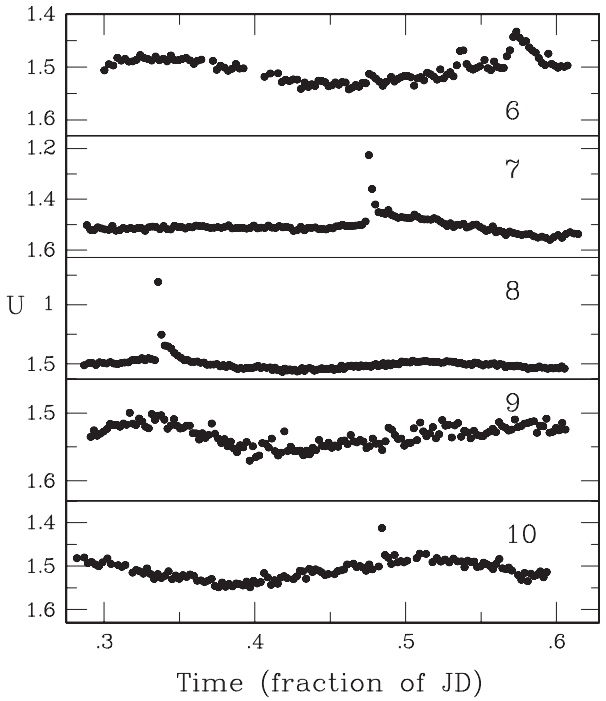

Figure 6. The data set 2 *U*-band CCD photometry. Each panel is labelled with the last digit of the Julian Day of the observations. Nightly magnitude zero-points were set by three bright stars in the field of view. Note the use of different vertical scales on the different panels.

light curves implies that there are no significant changes in the mean nightly brightness levels in *V* and *B*. Secondly, there are substantial flares visible in the *B*-filter data obtained during the second and third nights. The large flare on JD 245 5568 is echoed in the *V*-band data; with hindsight, the smaller flare near JD 245 5567.47 is also detectable in *V*. (It should be mentioned that the flares were consistently excluded in the fitting of periodicities to the data.)

The *U*-band data in Fig. 6 show flaring contemporaneous with the *B* band, but at substantially larger amplitudes. A short-lived flare near JD 245 5570.48, and a more extended, but low-amplitude event near JD 245 5566.57, do not have obvious counterparts at longer wavelengths.

The reader's attention is drawn to the fact that the mean *U*-band brightness level during JD 245 5569 is notably lower than that during the other four nights: it is also the only night without flaring activity.

Two runs were devoted to single filter observations, in order to monitor V760 for flaring activity: 4.7 h of Hα measurements and 4.4 h of *U*-band monitoring (the latter at a time resolution of 5 s), found only smooth variability on a time-scale of hours. Furthermore, no flares were seen in data set 3. This underlines the intermittency of the flaring activity: the reader is also reminded that about 36 h of time-series photometry obtained by Koen (2011) contained no overt signs of flaring.

Table 2 shows the results of fitting the four frequencies from Koen (2011) to data sets 2 and 3. In the case of data set 2, flares were first removed, and allowance was made for the nightly shifts in zero-point in *U* by setting all nightly mean magnitudes to zero. It is noteworthy that all data sets 2 and 3 amplitudes are considerably reduced from the data set 1 values found by Koen (2011). Amplitudes of different periodicities have not decreased by the same factors, neither are the reductions the same for the different filters. The greatest decrease is in the 5.053 d^{-1} variation: in the *V* band, this amplitude is factors of 3 and 2 smaller in data sets 2 and 3, respectively. The new amplitudes decrease monotonically with increasing wavelength, as expected if the variability is due to pulsation. This contrasts with data set 1, in which amplitudes in *B* and *V* were very similar. It is also noteworthy that the data set 3 amplitudes are markedly larger than the data set 2 values obtained two months earlier.

Fig. 7 shows spectra of the residuals after pre-whitening data sets 2 by the Table 2 frequencies. Maxima are 1.8 and 2.4 mmag, at 12.88 and 3.01 d^{-1}, for *V* and *B*, respectively. An apparent 3 d^{-1} periodicity is often seen in differentially corrected photometry of stars with extreme colours. It therefore seems likely that there is real variability in the *B* filter with this frequency, but that it is atmospherically induced. Pre-whitening the *B* residuals by 3.01 d^{-1} leads to

Table 2. Amplitudes obtained by fitting the frequencies 5.05336 and 3.62813 and their first harmonics to the observations. Data sets 2 and 3 are those obtained during the first (1.0 m) week and second (1.9 m) weeks logged in Table 1, while data set 1 results were taken from table 5 of Koen (2011). The uncertainty in the last digit of an entry is given in parentheses. Amplitude ratios are with respect to the *B*-filter values of the same data set: ratios for $f = 10.1068\,d^{-1}$ are not considered due to large uncertainties.

		Frequency (d^{-1})						
		5.0534	3.6281	7.2563	10.1068	5.0534	3.6281	7.2563
Filter	Data set	Amplitude (mmag)				Amplitude ratio		
U	2	17.3(6)	11.5(6)	6.1(6)	1.3(6)	1.08	1.21	1.20
	3	26.3(5)	14.0(5)	7.8(5)	1.5(5)	1.19	1.00	1.24
B	1	41.7(3)	15.7(3)	6.6(3)	1.6(3)			
	2	16.0(3)	9.5(3)	5.1(3)	0.8(3)			
	3	22.1(4)	14.0(3)	6.3(3)	1.8(3)			
V	1	41.1(5)	15.5(5)	6.5(4)	1.6(4)	0.99	0.99	0.98
	2	13.1(3)	8.7(3)	4.4(3)	0.6(3)	0.82	0.92	0.86
	3	19.8(2)	10.5(2)	5.0(2)	1.2(2)	0.90	0.75	0.80
R	1	35.8(5)	14.4(6)	6.2(4)	1.0(4)	0.86	0.92	0.94
	3	16.5(3)	9.1(3)	4.4(3)	0.8(3)	0.75	0.65	0.70
I	1	27.9(6)	13.0(6)	4.7(5)	2.1(5)	0.67	0.83	0.71

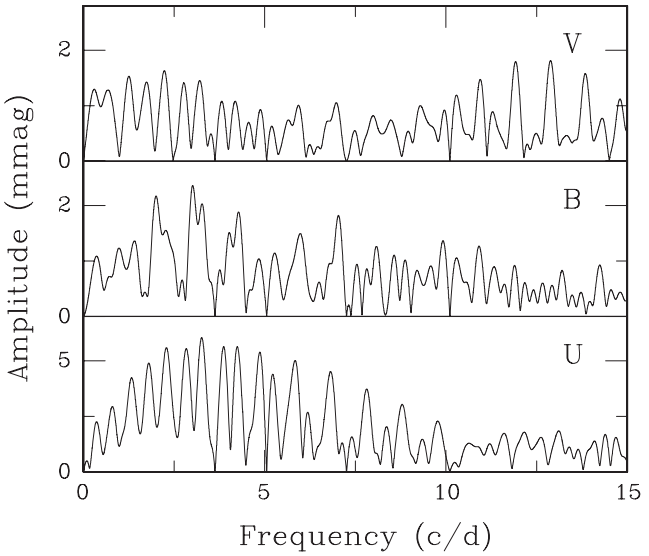

Figure 7. Amplitude spectra of the residuals left after pre-whitening the 1.0-m observations (data set 2) by the four frequencies in Table 2. Note the different scales on the vertical axes of the different panels.

a spectrum with a maximum of only 1.9 mmag, at a frequency of $3.26\,\mathrm{d}^{-1}$.

There is considerable power left in the data set 2 *U*-band spectrum after removal of the four frequencies in Table 2. Given the nature of the data, even after the flares have been excised, this is not surprising. Interestingly, the frequency at which the spectrum is maximum is also $3.26\,\mathrm{d}^{-1}$. This could be a coincidence, but is worth bearing in mind when analysing any future data.

The residual spectra of data sets 3 are plotted in Fig. 8. Frequencies close to (within $0.03\,\mathrm{d}^{-1}$) of $2\,\mathrm{d}^{-1}$ have been pre-whitened

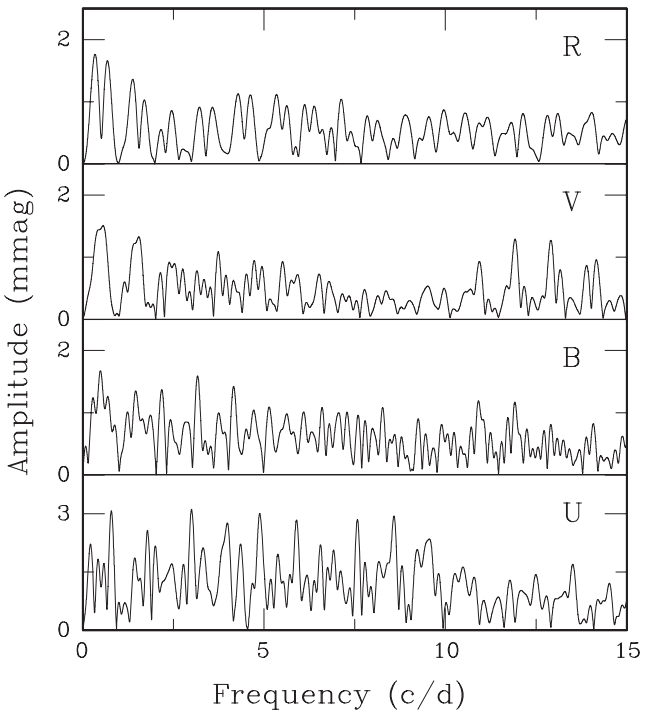

Figure 8. Amplitude spectra of the residuals left after pre-whitening the 1.9-m observations (data set 3) by the four frequencies in Table 2, and by one additional low frequency. Note that the vertical scale on the bottom panel is different from that on the other three panels.

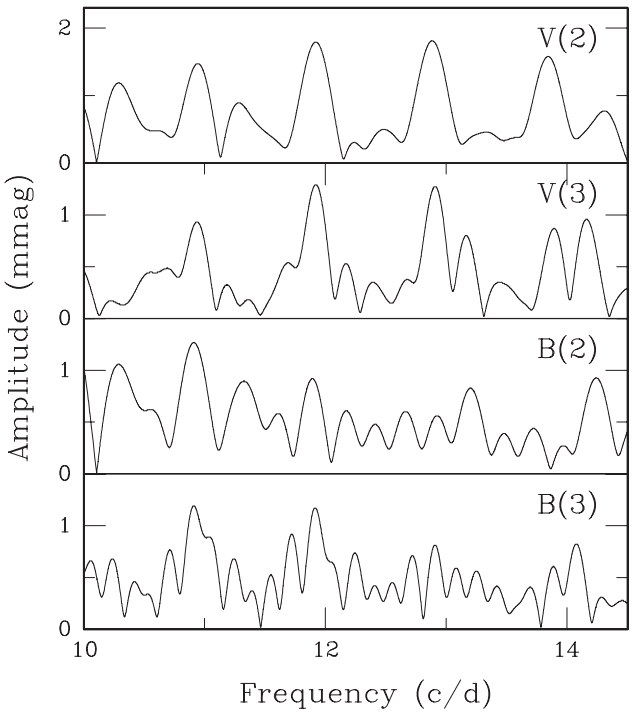

Figure 9. A comparison of the residual spectra of data sets 2 and 3 which show the possible presence of a new periodicity. The panels are labelled with the filter names; numbers in parentheses refer to the data set numbers.

from the *BVR* residuals, while $f = 0.93\,\mathrm{d}^{-1}$ has been pre-whitened from the *U* residuals. These low-frequency features are most likely artefacts due to nightly zero-point mismatchings. Comparison of the *V* data spectrum with that in Fig. 7 suggests that similar power excesses in the range 11–$14\,\mathrm{d}^{-1}$ are present in both data sets. A close look at the *B* data residual spectrum in Fig. 8 reveals two weak features in the same frequency range.

Fig. 9 shows, on an expanded scale, the spectra of the *V*- and *B*-filter residuals, for data sets 2 and 3. Clearly, there is a strong evidence for a common periodicity. The best agreement is at frequencies of $11.92\,\mathrm{d}^{-1}$ or 10.91–$10.94\,\mathrm{d}^{-1}$ (i.e. periodicities of 2.01 or 2.19–2.20 h). Amplitudes are in the range 1–2 mmag, being larger in *V* than in *B*.

The most plausible explanation of the periodicity is probably that the shape of the $3.628\,\mathrm{d}^{-1}$ variation deviates more from the sinusoidal than in 2010, and that the new frequency is the second harmonic at $10.88\,\mathrm{d}^{-1}$, in aliased form.

4 ASAS OBSERVATIONS

The time period covered by the UNSW observations of V760 was the 101 days JD 245 4086–245 4187, while the nine-night observation run of Koen (2011) took place almost 3 years later, during JD 245 5194–245 5212. The 'All Sky Automated Survey' (ASAS) obtained 707 *V*-band measurements during the interval JD 245 1868–245 5168. Of these, 620 data points are of reasonable quality (flags 1 and 2). Five observations are anomalously faint ($V > 12.55$), and are not used, leaving the 615 measurements plotted in Fig. 10.

The top panel of Fig. 11 shows an amplitude spectrum of the full data set: it is dominated by a prominent peak near $5\,\mathrm{d}^{-1}$, and its one and two cycles d^{-1} aliases. The spectrum maximum occurs at a frequency of $5.05292\,\mathrm{d}^{-1}$ (compared to $5.05336\,\mathrm{d}^{-1}$ derived by Koen 2011 from the UNSW data). The formal error in the ASAS

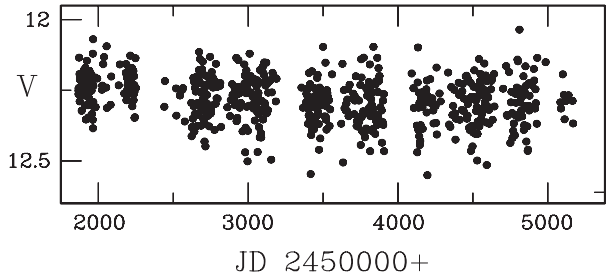

Figure 10. The ASAS photometry of V760.

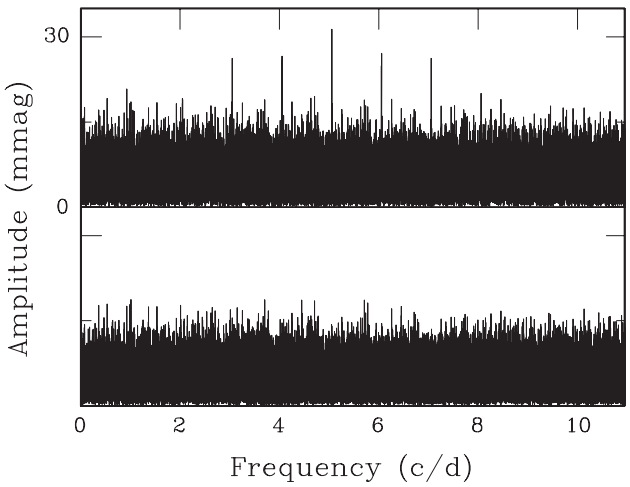

Figure 11. An amplitude spectrum of the ASAS data in Fig. 10 (top panel) and a spectrum of the residuals after pre-whitening by a frequency of 5.05292 d^{-1} (bottom panel).

Table 3. The subdivision of the ASAS data into four non-overlapping blocks.

Block number	Beginning date (HJD 245 0000+)	End date	Length (d)	Number of data points
1	1868	2251	383	105
2	2441	3189	748	171
3	3356	3907	551	151
4	4091	5168	1077	188

frequency is 2.2×10^{-5} d^{-1}, which is probably a severe underestimate in view of the further analysis presented below. Least-squares fitting of a sinusoid gives an amplitude of 32 mmag: pre-whitening by this fit leads to the featureless amplitude spectrum in the bottom panel of Fig. 11.

Study of subsets of the data leads to interesting new insights. Examination of Fig. 10 shows slight breaks in the data, roughly between observing seasons. The data were therefore split into four approximately continuous blocks – see Table 3 – and each was analysed separately. The amplitude spectra plotted in Fig. 12 demonstrate clearly that the 5.05 d^{-1} periodicity is not a fixed feature, underlining the message of Table 2. Note, in particular, that the noise levels of the spectra are much the same from data block to block. The reader's attention is also drawn to the fact that the highest peak in the bottom panel is at 3.6316 d^{-1} – very close to the 3.6281 d^{-1} frequency seen in the UNSW and SAAO data.

The highest peak in the block 2 spectrum is at 5.0528 d^{-1}, with a formal uncertainty of 1.1×10^{-4} d^{-1}. The amplitude of 51 mmag

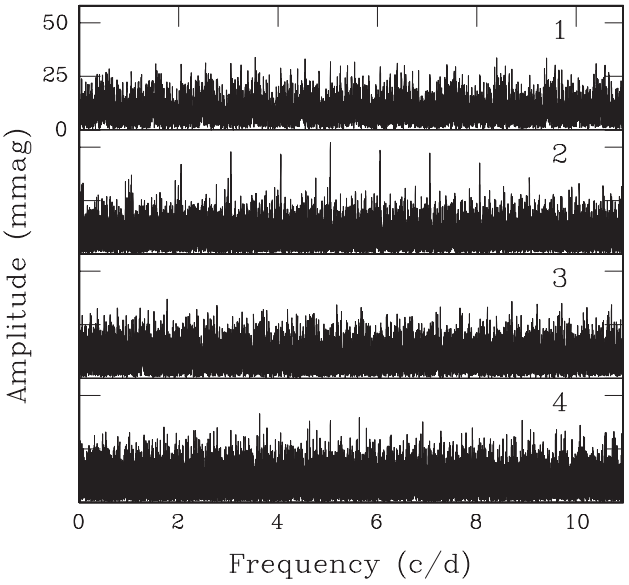

Figure 12. Amplitude spectra of the four consecutive sections of the ASAS photometry in Fig. 10.

seen in the block 2 ASAS data is the largest observed in V760 to date.

5 A CHANCE ALIGNMENT

A plausible explanation for the unusual combination of the physical properties of a late-type star, and the pulsational behaviour of an earlier type, is that the stellar image is made up of two components, with a projected positional difference substantially below an arcsecond. If the star with the earlier spectral type were a distant background object, it would contribute only a small percentage of the observed light, and if it were variable, the combined brightness would be modulated. Given the observed periodicities, candidate background variable types would be a double-mode RR Lyrae (RRd) star or a high-amplitude δ Scuti (HADS) star. There are, however, some arguments against this interpretation of the observations.

The presence of companion stars affects the relative amplitudes of a given pulsation mode, as measured through different filters. Klagyivik & Szabados (2009) used the effect to detect possible multiplicity in Cepheid variables. They recommend plotting amplitudes against inverse effective wavelengths of filters, and studying the slopes defined by the points. A large slope implies the presence of a red companion (variability in the blue more prominent), whereas a shallow slope implies a blue companion (variability in the blue less prominent).

Fig. 13 has amplitude plots for the dominant 5.05 d^{-1} mode in V760, for each of the three epochs of SAAO observations. The diagram shows that the slope of amplitude against inverse effective wavelength *increases* as the level of variability increases. This is the opposite of what is expected if the variability is due to a hidden blue companion. A larger level of variability would imply that the blue star is more prominent, the effect of the red contaminant (the K dwarf) reduced, hence the slope should decrease.

Koen (2009) presents an additional argument against close alignment of V760 with a background star. He studied time-series CCD photometry of unresolved images of close pairs of objects (separations <0.5 arcsec), and found that magnitudes determined from PSFs were strongly correlated with seeing. The effect appears to be

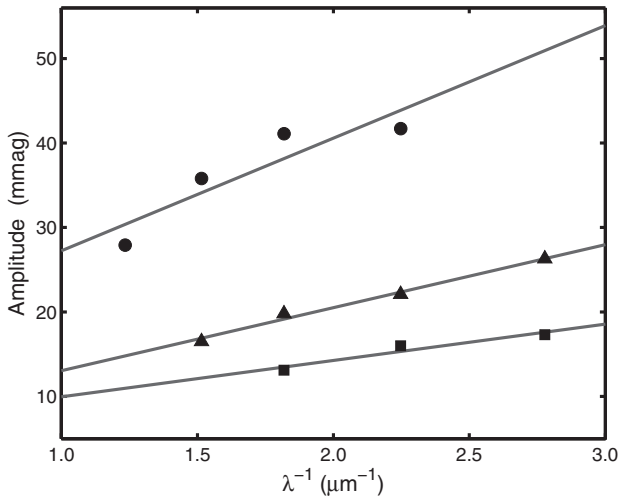

Figure 13. The wavelength dependence of the amplitude of the almost-sinusoidal variation ($f = 5.05\,\mathrm{d}^{-1}$) of V760, at three different epochs. Circles, squares and triangles respectively denote values derived from data sets 1, 2 and 3.

due to the fact that images are better modelled by Gaussian shapes under poor seeing conditions than when seeing is good (but still several times the separation between the components of the pair). In the case of V760, the PSF photometry has been unaffected by seeing, hence there is no indirect evidence for multiplicity of the images.

If the variability of V760 is due to chance alignment with a distant RR Lyrae star, then the latter has to be unique amongst such pulsators.

(i) If the longest period seen in V760 (0.276 d) is due to fundamental mode pulsation of an RR Lyrae star, then it is the shortest such period known. If furthermore the dominant period of 0.198 d is the first overtone, then the period ratio of 0.718 is the smallest known. These values can be compared to the Petersen diagram for Galactic bulge RRd stars recently published by Soszyński et al. (2011): the shortest fundamental period is 0.35 d, and the smallest period ratio 0.726. The authors ascribe these small values to the relatively high metallicity of the bulge stars. It is worth noting though that theoretical work by Szabó, Kolláth & Buchler (2004) showed that high-metallicity stars do not evolve through the double-mode region of the instability strip, therefore it is not clear that much smaller period ratios and fundamental periods are attainable.

(ii) Variations in the amplitudes of RR Lyrae are well known, in the form of the Blazhko effect (e.g. Smith 2006). However, it is clear that ASAS observations, with observable amplitudes in only one of the data blocks, do not fit the typical pattern of a periodic modulation of amplitudes. Furthermore, the author has been unable to find any mention of the Blazhko effect in double-mode RR Lyrae (see e.g. the review by Smith 2006).

Similar considerations apply if V760 is aligned with a HADS star.

(i) According to the review by McNamara (2000), in all double-mode HADS stars known at that time, the fundamental mode oscillation was dominant. In the case of V760, the shorter periodicity has the larger amplitude.

(ii) All known ratios of first overtone to fundamental mode period are larger than 0.74 (e.g. Pigulski et al. 2006; Poleski et al. 2010).

(iii) Fundamental mode periods of HADS are generally shorter than 0.25 d (e.g. Pigulski et al. 2006): in contrast, the longest period seen in V760 is 0.276 d.

(iv) To the best of the author's knowledge, amplitude modulation as observed in V760 has not been seen in any HADS star.

If there is indeed a distant star in almost exactly the same line of sight as V760, then it may be expected that the background star will have a different spatial motion. The proper motion of the K dwarf is of the order of 17 mas yr^{-1} (see Koen 2011). The implication is that images of the two stars should be easy to separate within a few decades.

6 FUTURE WORK

There are a number of avenues worth exploring.

(i) Imaging from a space telescope could help to answer the alignment question posed in Section 5.

(ii) High dispersion spectroscopy might also show whether variations originate in the K dwarf star, by the presence of radial velocity variations. Line profile variations could reveal modes which are not detectable by photometry.

(iii) Spectroscopy could also establish whether the star is very young, which again may explain its unusual properties.

(iv) Further time-series photometry of the star may help to establish whether there is any predictable pattern to the variations in the amplitudes of the periodicities. It would also be interesting to know the level of variability in the infrared: if it were appreciable, the case for the brightness changes being seated in the K dwarf star would strengthen.

ACKNOWLEDGMENTS

The author is grateful for telescope time made available at the South African Astronomical Observatory, and for the support of the SAAO technical staff. The author also thanks Dr Katrien Kolenberg for taking the time to answer a number of questions in detail, despite being in the midst of relocating to another continent; and Drs Patrick Lenz and Wojcek Dziembowski for suggesting the topic discussed in Section 5.

REFERENCES

Christiansen J. L. et al., 2008, MNRAS, 385, 1749
Klagyivik P., Szabados L., 2009, A&A, 504, 959
Koen C., 2009, MNRAS, 395, 531
Koen C., 2011, MNRAS, 411, 813
McNamara D. H., 2000, in Breger M., Montgomery M. H., eds, ASP Conf. Ser. Vol. 210, Delta Scuti and Related Stars: Reference Handbook and Proceedings of the 6th Vienna Workshop in Astrophysics. Astron. Soc. Pac., San Francisco, p. 373
Pigulski A., Kołaczkowski Z., Ramza T., Narwid A., 2006, Mem. Soc. Astron. Ital., 77, 223
Poleski R. et al., 2010, Acta Astron., 60, 1
Schechter P. L., Mateo M., Saha A., 1993, PASP, 105, 1342
Smith H. A., 2006, Mem. Soc. Astron. Ital., 77, 492
Soszyński I. et al., 2011, Acta Astron., 61, 1
Szabó R., Kolláth Z., Buchler J. R., 2004, A&A, 425, 627
Verner G. A. et al., 2011, MNRAS, 415, 3539

This paper has been typeset from a TEX/LATEX file prepared by the author.